Heat and Mass Transfer (2020) 56:2923–2937
https://doi.org/10.1007/s00231-020-02916-8

ORIGINAL

Experimental investigation of pressure drop and cooling performance of an automobile radiator using Al_2O_3-water + ethylene glycol nanofluid

Adnan Topuz[1] · Tahsin Engin[2] · Beytullah Erdoğan[1] · Serdar Mert[2] · Alper Yeter[3]

Received: 10 June 2019 / Accepted: 10 July 2020 / Published online: 14 July 2020

Abstract

In this study, the cooling capacity and the pressure drop variation in an automobile radiator using nanofluid instead of water with antifreeze that are investigated experimentally. The nanofluid consisted of 50% Ethylene Glycol–Water mixture including Al_2O_3 nanoparticles with 0.5% volumetric concentration was used as coolant. In all experiments, the inlet temperature of the cooling fluid into the radiator was held constant at 95 C. The tests were carried out at the air inlet temperature between 23.4–28.6 °C, the air velocity between 1.7–4.3 m/s, the cooling loads between 2.5–15 kW and the cooling fluid flow rates between 10 and 25 L/min. Results demonstrate that 50% Ethylene Glycol–Water based 0.5% vol. Al_2O_3 nanofluid increased the cooling capacity of the radiator up to 15% compared to the fluid with only 50% Ethylene Glycol–Water mixture. Instead of 15% increment, radiator can make with smaller surface area up to 15%, or the flow rate can be decreased for same heat transfer rate, so fluid pumping power consumption can be reduced in order to save fuel as much as pumping power economy. In addition, it has not been observed a remarkable increase in the pressure drop.

Keywords Al_2O_3 nanofluid · Cooling performance · Heat transfer enhancement · Pressure drop · Car radiator

Nomenclature

c	specific heat (J/kg · K.)
d	diameter (m)
EG	Ethylene glycol
EW	50% ethylene glycol–water mixture
k	thermal conductivity (W/m · K)
K	data of Kale Oto Radyatör for $V_{air}/V_{air,\ max}$
m	mass (kg)
$\dot{m}$	mass flow rate (kg/s)
N	(nanofluid)
P	pressure (bar, Pa)
Q	heat transfer rate (W)
T	temperature (°C, K)
V	velocity (m/s)
$\forall$	volumetric flow rate (m^3/s, L/min)
W	additional pumping power (W)
h	heat transfer coefficient (W/m^2K)

Greek symbols

α	thermal diffusivity (m^2/s)
Δ	variation or difference of a parameter
μ	dynamic viscosity (Pa · s) or (kg/m · s)
ρ	density (kg/m^3)
ϕ	volumetric concentration (%)

Subscripts

air	(air)
bf	base fluid
$cool$	(coolant)
EG	Ethylene Glycol
in	(inlet)
nf	(nanofluid)
np	(nanoparticle)
out	(outlet)
rad	(radiator)

✉ Beytullah Erdoğan
beytullah.erdogan@beun.edu.tr

[1] Engineering Faculty, Department of Mechanical Engineering, Zonguldak Bulent Ecevit University, Zonguldak, Turkey

[2] Engineering Faculty, Department of Mechanical Engineering, Sakarya University, Sakarya, Turkey

[3] Kale Oto Radyatör Sanayi ve Ticaret A.Ş, Kocaeli, Turkey

Table 1 Comparative table of literatures

Author	Base Fluid	Nano Particle	Concent-ration	Nanofluid Thermal Properties	Cooling Load	Air Inlet Velocity	Coolant Inlet Temp.	Coolant Inlet Flow Rate	Result
[5]	Water	GO, GNR	0.01–0.02% vol.	Measurement	2.5 kW	Variable	36–44 °C	0.6–0.9 m3/h	32% and 24.8% increment at total heat transfer coefficient for GO and GNR respectively
[9]	EG-Water	Al2O3	2–6% vol.	Measurement	–	–	–	–	3% increment at heat recovery efficiency
[15]	Water	Al2O3	0.2–1% vol.	Measurement	–	6–12 m/s	70–83.5 °C	0.109–0.384 L/s	83% increment at total heat transfer coefficient (at 34–35 °C Air Inlet Temp.)
[16]	Water	ZnO	0.01–0.3% vol.	Equation	6 kW	Constant	45–55 °C	7–11 L/min	46.5% increment at heat transfer
[17]	Water	TiO2	0.1–1% vol.	Equation	–	–	80 °C	90–120 L/min	45% increment at Nusselt number
[18]	EG-Water	Al2O3	0–1% vol.	Equation	2 kW	Variable	50–80 °C	16–18 L/min	40% increment at total heat transfer coefficient
[19]	EG-Water	CuO	0.05–0.8% vol.	Equation	18 kW	–	35–54 °C	4–8 L/min	55% increment at Nusselt number
[20]	Water	TiO2 SiO2	1–2% vol.	Measurement	1.5 kW	Constant	60–80 °C	2–8 L/min	55% increment at Nusselt number for TiO2 and SiO2 respectively
[21]	EG	Cu	0–2% vol.	Literature	–	–	70–95 °C	2–8 L/min	3.8% increment at heat transfer (at 27 °C Air Inlet Temp.)
[22]	Water	Fe2O3	0.15–0.65% vol.	Equation	6 kW	Variable	50–80 °C	3.33–8.33 L/min	13% and 11.5% increment at total heat transfer coefficient and heat transfer, respectively
[23]	Water	CuO Fe2O3	0.15–0.65% vol.	Equation	6 kW	Variable	50–80 °C	2.5–8.4 L/min	9% and 7% increment at total heat transfer coefficient for Fe2O2 and CuO, respectively
[30]	EG-Water	TiO2	0.1–0.5% vol.	Equation	–	Constant	35–45 °C	2–5 L/min	37% and 45% increment at heat transfer and Nusselt number, respectively
[31]	EG-Water	MW CNT	0.05–0.16% vol.	Measurement	–	Constant	50–80 °C	1.8–4.2 kg/min	17% decrement at heat transfer

Table 2 The properties of Al_2O_3 nanoparticle

Nanoparticle	Purity	Ave. particle diameter (nm)	Surface area (m^2/g)	Shape	Density (kg/m^3)	Specific heat ($J/kg \cdot K$)	Thermal conductivity ($W/m \cdot K$)
Al_2O_3	%99.8	13	85–115	Spherical	3890	778	46

*The values are taken from the manufacturer (Sigma–Aldrich) and the references numbered [34, 35]

1 Introduction

Efficiency at heat transfer has become one of the most important research subjects studied for years. Heat transfer is necessary in lots of applications such as cooling of electrical transformer, cooling of production workbench, air–condition systems in builds, heating and cooling processes of petrochemical, textile, paper, food, nuclear sectors, cooling of electronic devices and data centers, renewable energy like sun, geothermal [1–4]. And another important application of heat transfer is the cooling of vehicle engines. Because the engines transform approximately only one–third of the chemical energy into mechanical energy [5–7]. The remain energy is thrown from car as heat energy. Therefore, the engine cooling becomes crucial. However, day by day the engine power and size of vehicles increase, emission limits decrease, the engine manufacturers demand more cooling performance and less cooling volume. Those factors force energy engineers to produce more efficiency radiators that are the key component of the cooling system [8]. For more heat transfer rate, although the designers have developed effective methods like channels with rectangular cross–section, extended surfaces with fins, these methods have reached their limits (while the increase in heat transfer is 3% in the use of other methods, this value varies between 5% to 15% in the use of nano-fluids) and have started to be insufficient [9–14]. While a way to supply increased cooling loads is searched, nanofluid technology has appeared as a promising method. Nanofluid is a colloidal mixture obtained by adding powder particles with nanometer sized (<100 nm) inside a base fluid like water, oil [1, 9]. The object of using nanofluid is to improve the thermophysical properties of common cooling fluids used in radiators. Today in the literature, many studies on heat transfer using nanofluid can be found. Yet, it is accepted that the studies on nanofluids were started by Choi and Eastman firstly [3]. Then, application field of nanofluids has been widened toward various sectors. One of them was vehicle radiator. The studies about radiator have started to increase, recently. In this concept, some studies can be summarized as follows.

Kulkarni et al. [9] investigated cogeneration efficient of a 45 kW of diesel electrical generator using 50% EG–Water based Al_2O_3 nanofluid with 2–6% vol. concentration experimentally. Sankar [15] examined heat transfer increment in an experimental setup including a gasoline vehicle engine. He used water based Al_2O_3 nanofluid with 0.2–1% vol. concentration. The working conditions were 34–35 °C for air temperature and 6–12 m/s for air velocity, 70–83.5 °C for inlet temperature of cooling fluid and 0.109–0.384 L/s for its flow rate.Ali et al. [16] reported heat transfer increment in a car radiator. They used water based ZnO nanofluid with 0.01–0.3% vol. concentration. The working conditions were 45–55 °C for inlet temperature of cooling fluid. Bhimani et al. [17] inspected heat transfer increment in a car radiator. They used water based TiO_2 nanofluid with 0.1–1% vol. concentration.Bhogare et al. [18] controlled heat transfer increment in a car radiator. They used 50% EG–water based Al_2O_3 nanofluid with 0–1% vol. concentration. Heris et al. [19] conducted experiments to determine heat transfer increment in a car radiator using 60% EG–water based CuO nanofluid with 0.05–0.8% vol. concentration. Hussein et al. [20] investigated heat transfer increment in a car radiator using water based TiO_2 and SiO_2 nanofluid with 1–2% vol. concentration. Leong et al. [21] examined heat transfer and pumping

Table 3 Preparing conditions of nanofluid

Parameter	Value/Type
1. Ultrasonic power applied	500 W
2. Ultrasonic dispersing time	30 min
3. Height of ultrasonic probe from bottom	1–2 cm
4. Solution temperature	25 °C
5. Prepared solution volume in one process	500 mL
6. Nanoparticle and volumetric concentration	Al_2O_3 and 0.5%
7. Base fluid	50% EG–Su mixture
8. Water used in base fluid	Pure water
9. Ethylene glycol used in base fluid	Monoethylene glycol

Table 4 Masses of nanofluid components (for 25 °C)

Volumetric concent.	Nanofluid volume	Base fluid Density*	Particle density	Particle mass	Pure water Mass	Ethylene glycol Mass
Φ (%)	$\forall_{nf}$ (mL)	ρ_{bf} (kg/m^3)	ρ_{np} (kg/m^3)	m_{np} (g)	m_w (g)	m_{EG} (g)
0.5	500	1069.49	3890	9.72	248.00	284.06

*The base fluid is 50% EG–Water mixture and its thermophysical properties are taken from the company [33]

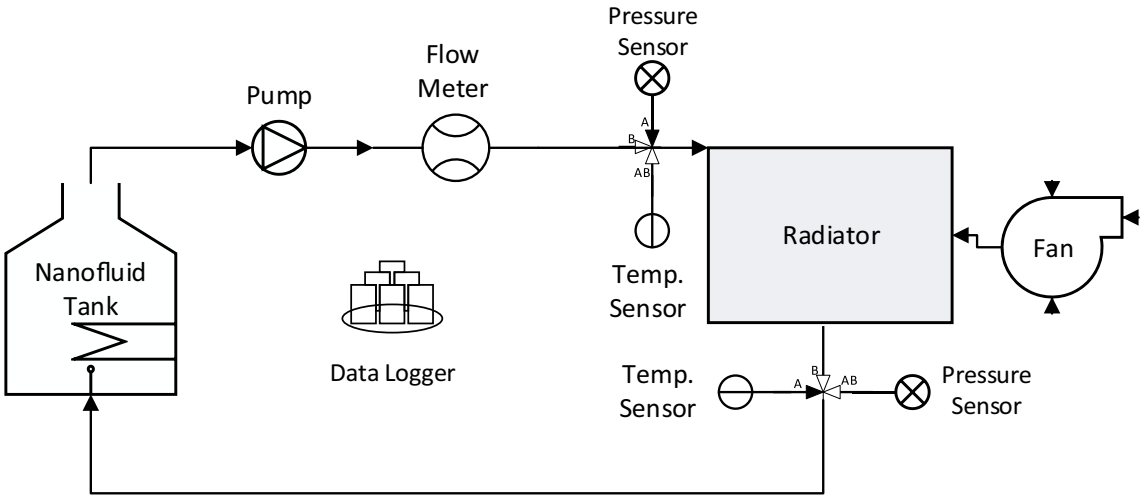

Fig. 1 Schematic diagram of the system

losses increment in a car radiator using EG based Cu nanofluid with 0–2% vol. concentration analytically.

Vermahmoudi et al. [22] reported total heat transfer coefficient increment in a car radiator using water based Fe_2O_3 nanofluid with 0.15–0.65% vol. concentration. The working conditions were 50–80 °C for inlet temperature of cooling fluid. Peyghambarzadeh et al. [23] researched total heat transfer coefficient increment in a car radiator using water based CuO and Fe_2O_3 nanofluids with 0.15–0.65% vol. concentration. The working conditions were 50–80 °C for inlet temperature of cooling fluid and 2.5–8.4 L/min for its flow rate. Kayhani et al. [24, 25] indicated that an experimental study of convective heat transfer and pressure drop of turbulent flow of TiO_2 (15 nm)-water nanofluid which are 0.1, 0.5, 1.0, 1.5 and 2.0% volume concentrations of nanoparticles. Results indicate that the enhancement of the Nusselt number is about 8% for nanofluid with 2.0% nanoparticle volume fraction at Re = 11,800.

The studies of Kayhani et al. [24] and Şahin et al. [1] are related to experimental investigation of laminar convective heat transfer and pressure drop of waterbased Al_2O_3 nanofluids in fully developed flow regime. Elias et al. [14] experimentally examined heat transfer and pressure drop in a plate heat exchanger with 30° and 60° chevron angles by using Al_2O_3 – water nanofluid. Duangthongsuk and Wongwises [26] worked an experimental study on the heat transfer performance and pressure drop of TiO_2–water nanofluids flowing under a turbulent flow regime. Nazari et al. [27, 28] investigate the CPU cooling using Alumina and CNT nanofluids and comparing the cooling performance of the common base fluids.

Maghrebi et al. [29] showed the effects of flow and migration of nanoparticles on heat transfer in a straight channel occupied with a porous medium by using the fully developed flow and steady Darcy–Brinkman–Forchheimer equation in porous channel. The effects of parameters such as Lewis number, Schmidt number, Brownian diffusion, and thermophoresis on the heat transfer are completely studied.Sandhya et al. [30] inspected convection heat transfer coefficient increment in a car radiator using 40% EG–water based TiO_2 nanofluid with 0.1–0.5% vol. concentration. The working conditions were 35–45 °C for inlet temperature of cooling fluid and 2–5 L/min for its flow rate. Oliveira et al. [31] controlled temperature drop and heat transfer increment in a car radiator using EG–water based MWCNT nanofluid with 0.05–0.16% wt. concentration. The working conditions were 0.175 kg/s for air flow rate, 50–80 °C for inlet temperature of cooling fluid and 1.8–4.2 kg/min for its flow rate,

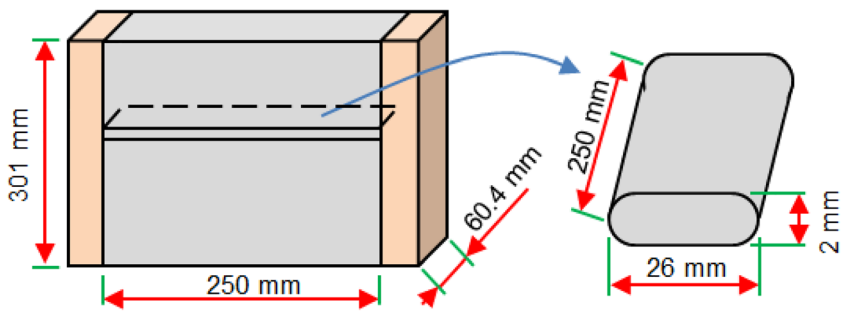

Fig. 2 Radiator dimensions of the system

Table 5 Properties of the radiators

Type	a) R1	b) R2
Mark / Model	KALE / ABB	KALE / Peugeot
Core Dimensions Width x Height x Depth	228 × 196.4 × 45 mm	250 × 301 × 60.4 mm
Channel Dimensions–Outer Side (Height x Width)	3 × 36 mm	2 × 26 mm
Channel Thickness	0.6 mm	0.5 mm
Channel Dimensions–Inner Side (Height x Width)	1.8 × 36 mm	1 × 25 mm
Channel Hydraulic Diameter	~3.4 mm	1.923 mm
Number of Channel	16	34
Pitch of Channel (Fin/Inch)	10 fpi	20 fpi
Channel Type	Louver	Louver
Channel and Fin Material	Aluminum	Aluminum

constant air velocity. Emerald et al. [32] investigated the heat transfer performance and entropy analysis for heat pipe (CLHP) with Al_2O_3/water and Ag/water nanofluid (volume concentrations of 0.09% and 0.12%). Heat pipe has been fabricated and tested for from 30 to 500 W. The experimental tests are for Al_2O_3 nanoparticles, an enhancement of 34.52%, 23.7%, 39.27% and 30.8%, respectively, 15% when compared with that of Al_2O_3/water nanofluid against Ag. As a result, it was concluded that each nanofluid is not proper for cooling systems.It can be seen that the literature studies above mentioned include one or more of the following findings:

1. Each study could not be conducted at real operating conditions of coolant around 85–95 °C [5, 33].
2. If the tests were conducted at real operating conditions, the nondimensional numbers such as Nusselt and Reynolds could not be calculated correctly. Due to high deviations of measurement devices used, it is difficult to measure thermal conductivity and viscosity of nanofluid at high temperatures close to 95 °C.
3. The equations in the literature used for thermal conductivity and viscosity of nanofluids are more suitable for lower temperature degrees than 50 °C.
4. Since resistance power as cooling load are not enough, it was studied at low levels for coolant fluid flow rate.
5. Since coolant fluid inlet temperature does not decrease, it was studied at low levels for air flow rate.
6. The air velocity sent to radiator was held as constant. Thus, the effect of the air velocity variation on radiator performance could not be seen.
7. No information was given for air inlet temperature. It is the most effective factor on radiator performance.

Table 6 Test conditions of the validation radiator

Cooling fluid	50% EG–Water
Channel size	Inner: 3 × 36 mm, Thickness: 0.6 mm
Number of channel and core size	16–228 × 196.4 × 45 mm
Cooling load	2.5–15 kW
Coolant fluid inlet temperature	95 °C
Coolant fluid flow rate	19–21 – 23 – 25 L/min
Air velocity	4.3–7.9 – 11.2 – 12.9 m/s
Air inlet temperature	min. 27.2 °C – max. 29.6 °C

As there is no sufficient study for the real operating conditions of a car radiator, in this study, those conditions are considered. Furthermore, almost all studies obtained maximum heat transfer increments at maximum volume concentrations. For that nanofluid as coolant fluid can become popular, also it has to be taken into account that it must be affordable. In this investigation, 50% Ethylene Glycol–Water based Al_2O_3 nanofluid with 0.5% volumetric concentration was prepared as coolant to determine heat transfer rate enhancement and pressure drop in car radiator. In addition, the originality of this study is the experiment under real working conditions up to 95 °C and, that compared with the company. Also, the prototype radiator produced in this study has been tested by KALE for a long time (Table 1).

2 Material and METOD

2.1 Preparation of nanofluids

It is necessary for the nanofluids prepared to become stable and homogenous to diminish some problems: Agglomeration, clogging in a channel and poor heat transfer performance. For this purpose, the stability and homogeneity controls of the nanofluid have to be examined after preparing them. It was used Al_2O_3 as nanoparticle and 50% ethylene glycol–50% pure water as base fluid. The properties of the Al_2O_3 nanoparticles are given in Table 2.

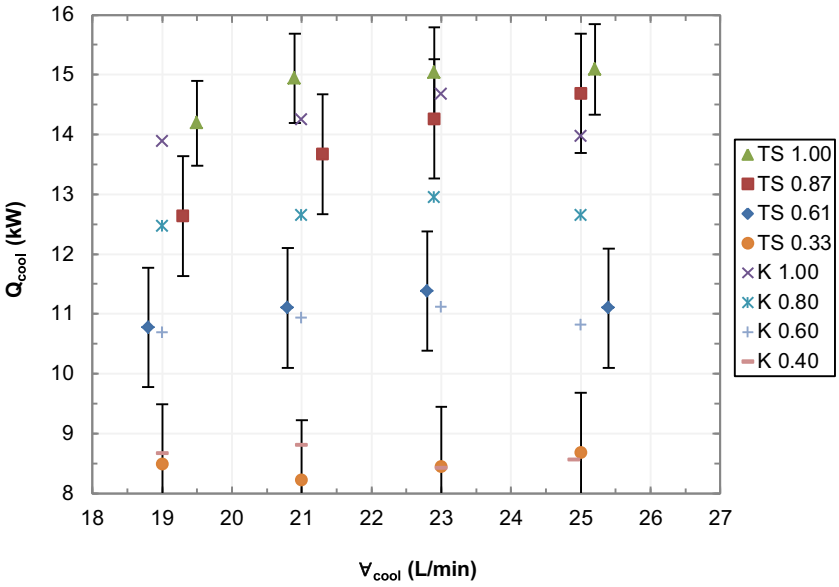

Fig. 3 Cooling capacity variation of the cooling fluid (used error rate ±5%) (TS: This Study, K: data of Kale Oto Radyatör for $V_{air}/V_{air,max}$)

The nanofluid used in this study was prepared by 2–step method. Mass amounts of the nanoparticles and 50% EG–Water base fluid were weighted by a precision balance (AND GX–600, Max: 610 g, Deviation: 0.001 g). After the Al_2O_3 nanoparticles were added into 50% EG–Water base fluid in a flask, the flask was placed inside a heat bath with temperature–controlled (Cole Parmer/EW–12108–25, Temperature: -20 ~ 200 °C, Bath Capacity: 6 L, Heating Power: 1 kW, Cooling Power: 200 W, Flow Rate: 11 ~ 24 L/min) [36]. Here, the mixture was sonicated by a probe type of ultrasonic homogenizer to prevent the agglomeration of the nanoparticles and to disperse them homogeneously in base fluid (Optic Ivymen System/CY–500, Power: 500 W, Frequency: 20 kHz, Probe Diameter/Length: Ø5.6/60 mm). No surfactant was used. The preparing conditions of nanofluid can be summarized in Table 3, and the mass amounts to prepare a 500 mL of nanofluid are given in Table 4.

The stability of the nanofluid enabled up to 5 days for Al_2O_3, so no need stability during testing. Also, the nanofluid was investigated by photo–capturing method and their homogeneity and geometry (Spherical) were controlled by SEM (Scanning Electron Microscope) and TEM (Transmission Electron Microscope) images. 3 different concentration ratios (0.5,0.7,1.0%) were studied in the previous study. When 3 concentration ratio was used, the cooling loads were similar. Lower volumetric concentration was chosen to prevent the radiator channel from blocking [37].

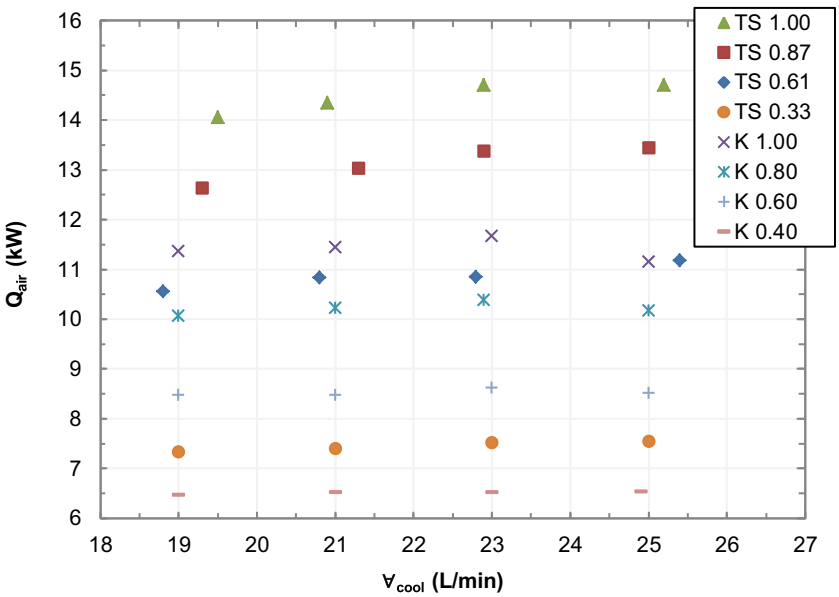

Fig. 4 Cooling capacity change of the air

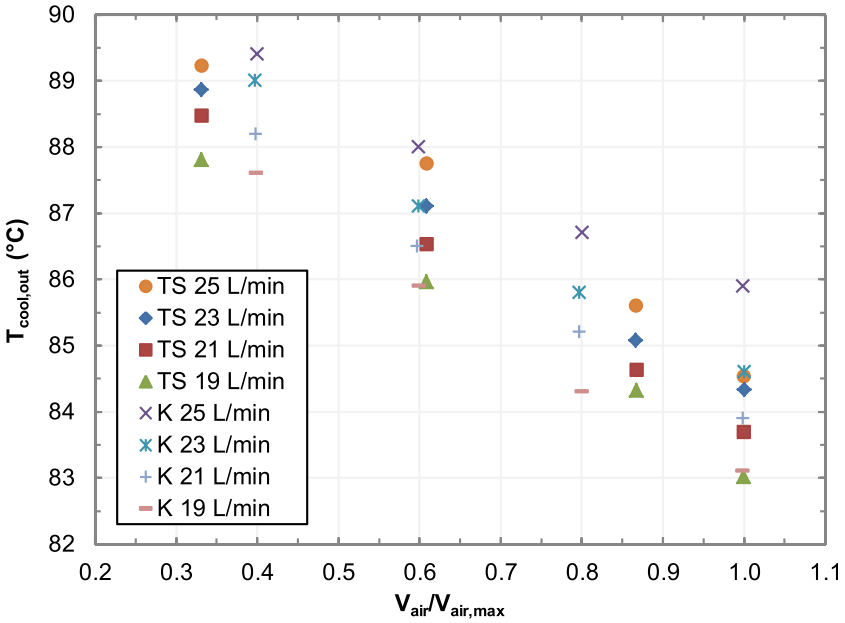

Fig. 5 Temperature change of the coolant fluid

2.2 Thermophysical properties of nanofluids

In the calculations, the Eq. (1) and (2) are used for the density and the specific heat. The thermal conductivity and the viscosity of the nanofluid were separately measured for each volumetric concentration respectively. When the experimental results were compared with Eq. 3 and 4, very close values were found. Therefore, Eq. (3) and (4) are used for the thermal conductivity and the viscosity [38].

$$\rho_{nf} = \rho_{np}\phi + \rho_{bf}(1-\phi) \tag{1}$$

Where ρ is density; ϕ is volumetric concentration; *nf*, *np*, *bf* are nanofluid, nanoparticle and base fluid indices, respectively.

$$c_{nf} = \frac{\rho_{np}c_{np}\phi + \rho_{bf}c_{bf}(1-\phi)}{\rho_{nf}} \tag{2}$$

Where c is specific heat.

$$\frac{k_{nf}}{k_{bf}} = 0.8938 \cdot (1+\phi)^{1.37} \cdot \left(1+\frac{T_{nf}}{70}\right)^{0.2777} \cdot \left(1+\frac{d_{np}}{150}\right)^{-0.0336} \cdot \left(\frac{\alpha_{np}}{\alpha_{bf}}\right)^{0.01737} \tag{3}$$

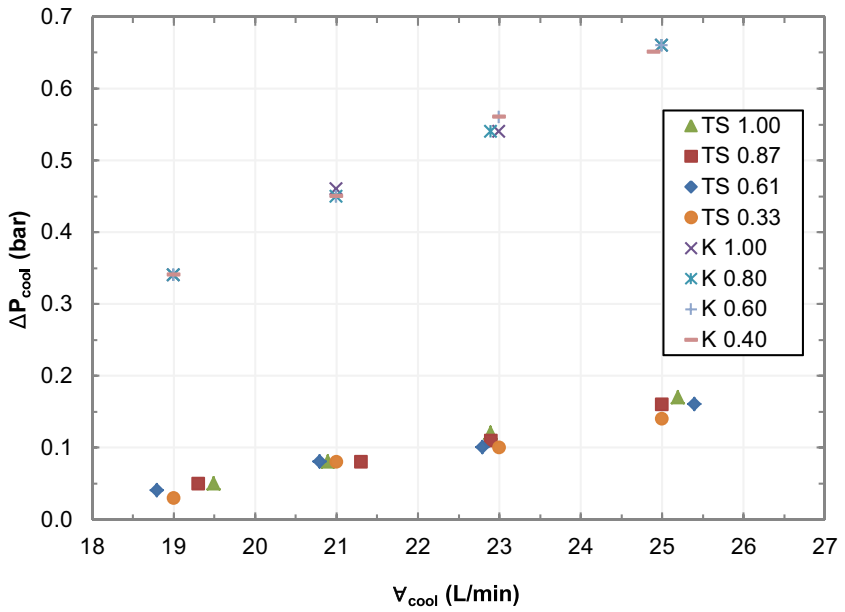

Fig. 6 Pressure drop of the coolant fluid

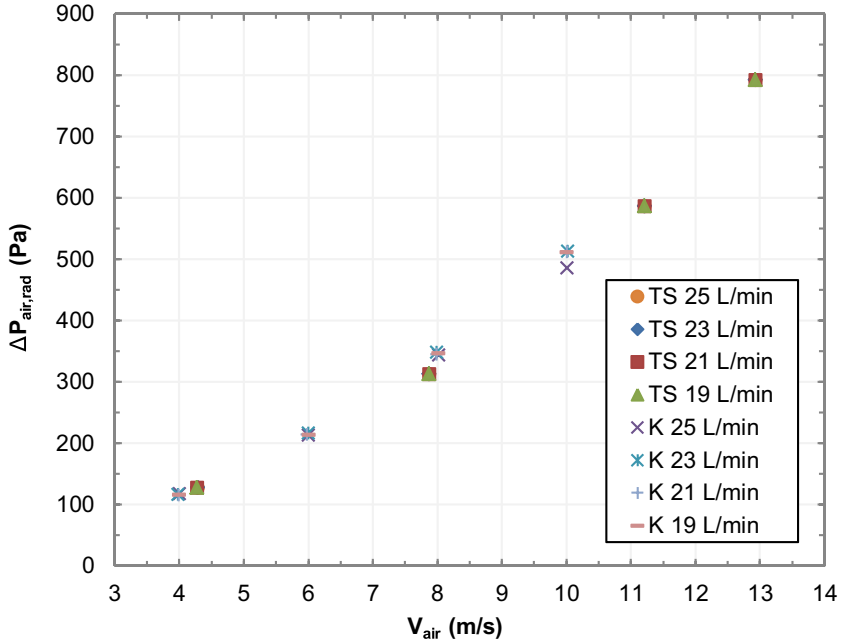

Fig. 7 Pressure drop of the air

Where k is the thermal conductivity; T is the temperature in Celcius; d is the diameter of the nanoparticle in nm; α is the thermal diffusivity that is equal to $k/\rho c$, respectively.

$$\frac{\mu_{nf}}{\mu_{bf}} = (1+\phi)^{11.3} \cdot \left(1+\frac{T_{nf}}{70}\right)^{-0.038} \cdot \left(1+\frac{d_{np}}{170}\right)^{-0.061} \quad (4)$$

And where μ is the dynamic viscosity. The thermophysical properties of 50% EG–Water mixture are given between Eqs. (5)–(8). Those equations are obtained by the curve fittings for the data between 0 and 120 °C taken from the company [33]. The maximum deviations for these equations are 0.03%, 0.10%, 0.01% and 1.45% (0.92% for 0–100 °C) for the density, the specific heat, the thermal conductivity and the viscosity, respectively. Where T is the temperature in Kelvin.

$$\rho_{bf} = -0.00145 \cdot T^2 + 0.30610 \cdot T + 1107.33704 \quad (5)$$

$$c_{bf} = -0.0236 \cdot T^2 + 19.907 \cdot T - 495.09 \quad (6)$$

$$k_{bf} = -0.00000000004162 \cdot T^2 + 0.00062900433445 \cdot T + 0.20727014595915 \quad (7)$$

$$\mu_{bf} = -0.00000070.T4 + 0.00088431.T3 - 0.41635244.T\,2 + 86.99864018.T - 6,805.63 \quad (8)$$

3 Experimental setup

For the performance measurements, the schematic diagram and the image of the experimental system were constructed

Table 7 Test conditions of the prototype radiator

Cooling fluid	Nanofluid or 50% EG–Water
Radiator type	Peugeot (R2)
Channel size	Inner: 1 × 25 mm, Thickness: 0.5 mm
Number of channel	34
Core size	250 × 301 × 60.4 mm
Cooling load	2.5–15 kW
Cooling fluid inlet temp.	95 °C
Cooling fluid flow rate	10–15 – 20 – 25 L/min
Air velocity	1.7–2.4 – 3.4 – 4.3 m/s
Air inlet temperature	min. 23.6 °C – max. 28.6 °C (for Nanofluid)
	min. 23.4 °C – max. 24.9 °C (for 50% EG–W.)

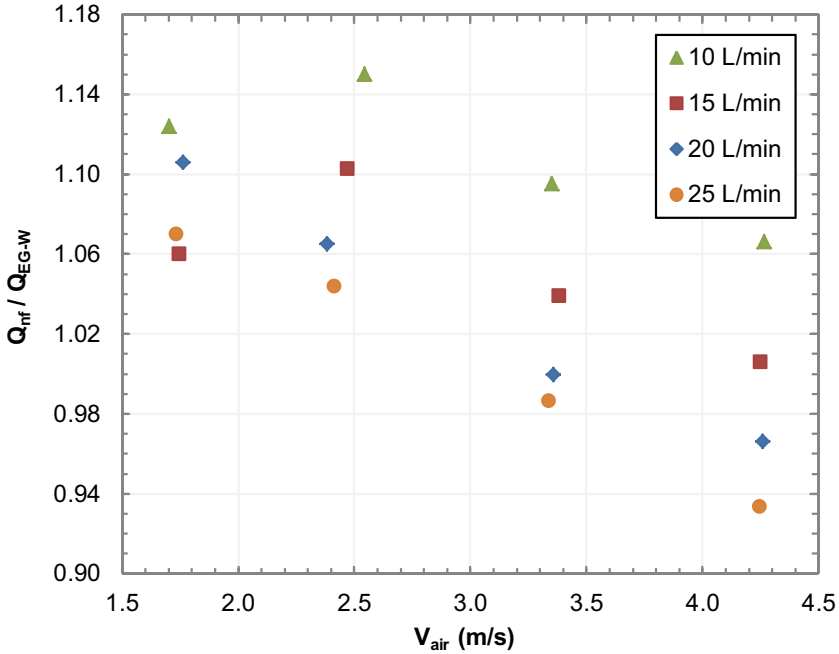

Fig. 8 Cooling capacity variation of the nanofluid according to 50% EG–Water mixture

that are shown in Fig. 1. The setup composes of a fluid tank, two resistances, valves, a centrifugal pump, an electromagnetic flow meter, temperature sensors, pressure sensors, a car radiator, two differential manometers, air channels, a centrifugal fan, a data logger, an electrical control panel, a frequency converter, pipes and fittings (Fig. 2).

The pump (Pentax, Ultra 3S–100–5, up to 80 L/min) takes the fluid from the fluid tank, sends it to the radiator by passing inside the flow meter with accuracy of 0.4% of reading (ABB, FEH311, 1–90 L/min) to measure its flow rate and makes it return to the fluid tank. The fluid flow rate is controlled by two valves located at the outlet of the pump. The fan (Eurovent, EU 352, gives 3780 m^3/h at 981 Pa total pressure) used to supply to the radiator the air is controlled by the frequency converter (Siemens, Micro Master MM550–3, 5.5 kW) that enables the air velocity control by changing the revolution of the fan. Here, the fluid tank with 130x240x240 mm sized (base x height) is full up to approximately 10 cm height to cover the resistances in the tank. Two resistances with a 15 kW of total heating power (each of them has 3 × 2.5 kW power, 220/380 V) are used to model the cooling load of an engine. A thermostat (Enda, ET5412) controls the resistances in order to increase the inlet temperature of the fluid into the radiator to the desired temperature. The NTC temperature

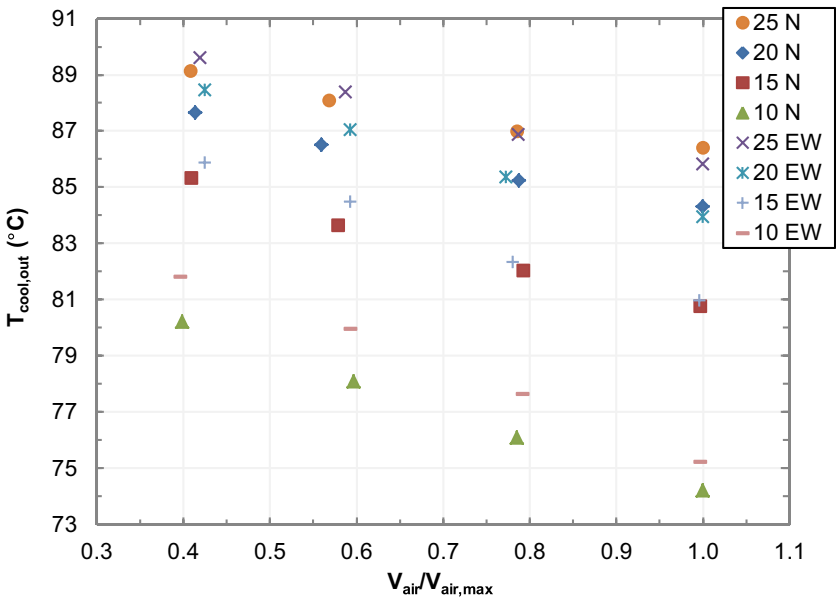

Fig. 9 Temp. variation of the nanofluid according to 50% EG–Water

Table 8 Calculation Nu_{ave} by using performance radiator R2 for base fluid and nanofluid

Parameters	Base fluid				Nanofluid			
$\forall_{cool}$ (L/min)	10.0	15.0	20.0	25.0	10.0	15.0	20.0	25.0
$T_{cool,in}$ (°C)	94.8	94.9	95.0	95.1	95.0	95.1	95.0	95.0
$T_{cool,out}$ (°C)	79.9	84.5	88.5	89.6	78.1	83.6	87.7	89.1
$T_{air,in}$ (°C)	24.3	23.9	23.6	23.6	24.2	25.6	26.2	27.5
$T_{air,out}$ (°C)	54.9	56.3	58.0	58.6	52.4	55.4	57.9	58.8
$T_{surface}$ (°C)	63.5	64.9	66.3	66.7	62.4	64.9	66.6	67.6
ρ_{cool} (kg/m^3)	1029	1027	1025	1025	1044	1042	1041	1040
c_{cool} (J/kgK)	3614	3621	3626	3628	3559	3567	3572	3574
k (W/mK)	0.44	0.44	0.44	0.44	0.45	0.44	0.43	0.42
h (W/m^{2}K)	5250	5300	4303	4397	6028	5948	4927	4934
Nu_{ave}	22.94	23.16	18.81	19.22	25.48	26.07	22.14	22.39

sensors with accuracy of ±1.02 °C (Vishay, NTCLE300E3103SB, −40 ~ +125 °C) and the pressure sensors with accuracy of 0.4%/10 K (for >20 °C) of full scale (ITEC, P103, 0–1 bar) were used to measure the fluid temperature and its pressure. The thermocouples (Elimko, MI04–1 K30–10–K20, K type) were used to measure the air temperature. The data logger (MC, IOTech Personal DAQ 3000) was used to read and save the temperature data. The differential manometers with accuracy of 1% of reading (Testo, 350 M/XL–454, 0–200 mbar) were used to measure the velocity of the air by a pitot tube and its pressure drop in the radiator.

In the present study, each experimental study was repeated three times and two radiators were used [39]. One of them was for calibration and verification of the results, the other was for the performance tests. The properties of the radiators are given in Table 5. All devices in the experimental setup are chosen in a way to be durable to at least 110 °C temperature. The performance experiments were conducted at cooling fluid flow rates of 10, 15, 20, 25 L/min, at air velocities of 1.7, 2.4, 3.4, 4.3 m/s, at cooling fluid inlet temperature of 95 °C, at air inlet temperature changing between 23.4 °C and 28.6 °C, and the cooling loads between 2.5 and 15 kW.

3.1 Data reduction

The average of the inlet and the outlet temperature was used to determine the thermophysical properties of the fluid. The heat transfer rate the coolant fluid rejects was calculated from Eq. (9) and (10),

$$Q = \dot{m} c_p (T_{out} - T_{in}) \tag{9}$$

$$\dot{m} = \rho \dot{\forall} \tag{10}$$

where Q is heat transfer rate; $\dot{m}$ is mass flow rate; c_p is specific heat, T_{out} and T_{in} are outlet and inlet

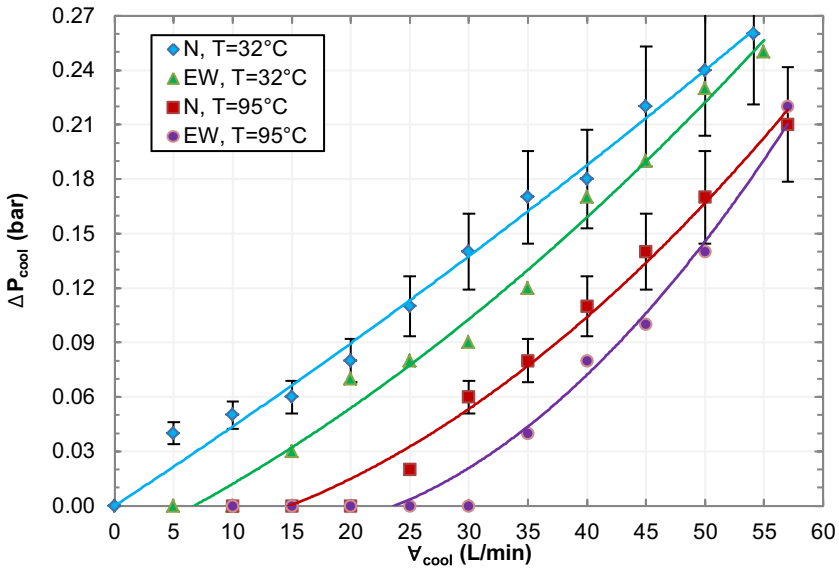

Fig. 10 Pressure drop of the nanofluid according to 50% EG–Water (used error rate ±15%)

temperatures of the coolant fluid from and into the radiator; ρ is density and $\dot{\forall}$ is flow rate.

Convection heat transfer coefficient,

$$Q = hA_s\Delta T_{ln} \tag{11}$$

$$A_s = \pi D_{in} L \tag{12}$$

$$\Delta T_{ln} = \frac{\Delta T_{in} - \Delta T_{out}}{ln(\Delta T_{in}/\Delta T_{out})} \tag{13}$$

$$\Delta T_{in} = T_{in} - T_{s,in} \tag{14}$$

$$\Delta T_{out} = T_{out} - T_{s,out} \tag{15}$$

where h is average convection heat transfer coefficient, A_s is surface area, ΔT_{ln} is logarithmic average temperature difference, $T_{s,\,in}$ and $T_{s,\,out}$ are inner surface temperatures at inlet and outlet, respectively.Pressure drop and additional pumping power are calculated according to Eq. (16) and (17) which are;

$$\Delta P_f = f\frac{L}{D_{in}}\frac{\rho V^2}{2} \tag{16}$$

$$W = \dot{\forall}\, x\, \Delta P_f \tag{17}$$

ΔP_f is friction pressure drop, f is friction factor, L is length, D_{in} is diameter of radiator, ρ is fluid density, V is fluid velocity, W *is* additional pumping power and $\dot{\forall}$ is flow rate.

4 Results and discussion

4.1 Validation experiments

Before starting the experiments, the validation of experiments were conducted to confirm the reliability of the results obtained. This process was done by comparing the experimental results with the company's ones for a radiator known the performance results. The company has a laboratory that is approved by the automotive companies like Renault and Fiat. The nanofluid experiments were carried out with only 8 L volume at the university laboratory since about 400 L volume of nanofluid was necessary to test with the company's facilities. Preparing such an amount of nanofluid takes a long time and is not affordable.The test conditions were chosen the company's conditions as close as possible. For only the air temperature could not be controlled, the different conditions for air temperatures and velocities had to be used. The test conditions are given in Table 6. The results obtained at these conditions are given between Figs. 3 and 7.

Since the air inlet temperatures at the test conditions were not same as those of the company, the fan revolution and air flow rate was increased to enable same coolant fluid outlet temperature. The air velocities and inlet temperatures were higher than the company's data (The air inlet temperatures were 25 °C for the company's data). Furthermore, it was seen that measuring of the air outlet temperature was difficult since the air outlet temperatures are not homogeneous and it can change according to the air velocity. That is why the heat the air taken was different from that of the company's.To compare the Kale and this study data, ratio of air velocity of

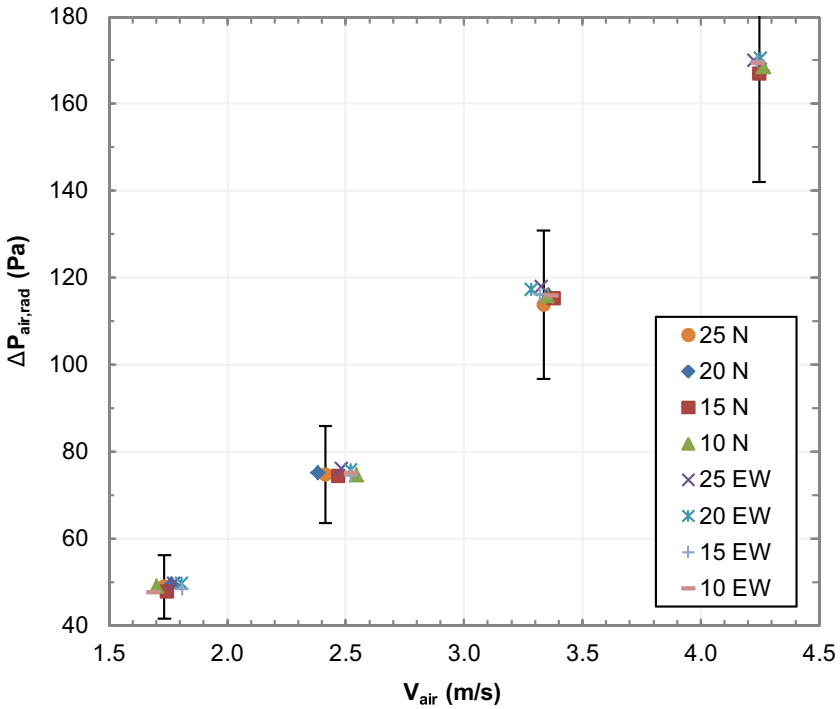

Fig. 11 Pressure drop of the air (N: Nanofluid, EW:E.Glycol-Water) **(used error rate ±15%)**

Table 9 Uncertainties of variables measured

No	Instrument	Range	Variable measured	Total uncertainty	Values in experiment		Uncertainty	
					Min	Max	Min	Max
1	NTC Temperature Sensor (Vishay, NTCLE300E3103SB)	−40 ~ 125 °C	Fluid inlet temperature, T_{in}	$U_{Fixed,T_{in}} = \pm 1.02°C\ U_{T_{in}}$ $= \sqrt{U^2_{Fixed,T_{in}} + U^2_{Random,T_{in}}}$ $= \sqrt{1.02^2 + 0^2} \cong \pm 1.02°C$	T_{in} (°C) 94.8	95.1	$U_{T_{in}}/T_{in}$ 1.0726%	1.0759%
2	NTC Temp. Sensor	−40 ~ 125 °C	Fluid outlet temperature, T_{out}	$U_{T_{out}} = \sqrt{1.02^2 + 0^2} \cong \pm 1.02°C$	T_{out} (°C) 74.2	89.6	$U_{T_{out}}/T_{out}$ 1.1384%	1.3747%
3	Pressure transmitter (ITEC, P103)	0 ~ 1 bar	Pressure drop, ΔP	$U_{\Delta P} = 1 \times \frac{0.4\%}{10\ K} \times (90-20)$ $\cong \pm 0.028\ bar$	$\Delta P\ (bar)$ 0	0.22	$U_{\Delta P}/\Delta P$ 12.727%	–
4	Flow meter (ABB, FEH311,)	1 ~ 90 L/min	Volume flow rate, $\dot{\forall}$	$U_{\dot{\forall}} = \sqrt{0.1^2 + 0^2} \cong \pm 0.1\ L/min$	$\dot{\forall}\ (L/min)$ 10.0	25.0	$U_{\dot{\forall}}/\dot{\forall}$ 0.04%	1.0%
5	Thermophysical properties	Density, ρ Specific heat, c_p		$U_\rho/\rho = \sqrt{(0)^2 + (0)^2 + (0.03\%)^2} = \pm 0.03\%$ $U_{c_p}/c_p = \sqrt{(0)^2 + (0)^2 + (0.10\%)^2} = \pm 0.1\%$				

maximum air velocity ($V_{air}/V_{air,\ max}$) was used in Fig. 3. It can be seen in Fig. 3 that while the coolant fluid flow rate is increased, the cooling load is increased, but after 23 L/min flow rate of coolant fluid, cooling load is being decreased. Same tendency is seen between Kale and this study.In the Fig. 4, cooling capacity of the air was investigated. While coolant fluid flow is usually increased, cooling capacity of the air is increased. Ratio of air velocity ($V_{air}/V_{air,\ max}$) is increased, outlet temperature of the coolant fluid is decreased as seen in Fig. 5. In the Fig. 6, flow rateof coolant fluid is increased, pressure drop of thecoolant fluid is increased. Figure 7 shows that sane increment can be seen for pressure drop of the air.

As mentioned above that, same results are obtained between Kale and this study validation experiments, and then performance experiments were started with other radiator. The differences and similarities between Kale radiator and this study are as follows: The radiator previously tested by Kale has been retested with the installed experimental setup and calibration tests have been performed.Cooling Fluid pressure tests, air velocity-pressure tests, cooling fluid and air temperature tests were performed. Differences were observed in the cooling fluid pressure tests. The causes of these differences were investigated. The type and location of the pressure sensors (manuel and digital) have been changed, the measurement location has been changed and different antifreezes have been tested. In addition, the measurement accuracy of the electromagnetic flowmeter was investigated. As a result, the deviation in the pressure values of Kale; reading error or device error. Then, air velocity and pressure drop tests were obtained at the same fluid flow rates close to Kale's data. Finally, temperature tests were performed for fluid and air, and similar results were obtained with Kale. After these stages, performance tests were performed with the existing radiator and the newly designed prototype radiator for this study.

4.2 Performance results

After the validation experiments, the prototype radiator (Peugeot, R2) tests were conducted. This process was done by comparing the experimental results obtained by using the nanofluid with the those of 50% EG–Water mixture. The air velocity and the fluid flow rate were chosen in a way to enable a 95 C of fluid temperature at the radiator inlet. The test conditions and the results obtained at these conditions are given in Table 7 and between Figs. 8 and 11.

The following results are found:

1. It has been concluded that the usage of nanofluids with proper nanoparticles and concentrations could lead to improvement in the cooling performance of the radiator by 15%. The test conditions are 10 L/min for fluid flow

Table 10 Uncertainty of results calculated

	Result	Maximum uncertainty
1	Mass flow rate, $\dot{m} = \rho\dot{\forall}$	$\frac{U_{\dot{m}}}{\dot{m}} = \left[\left(\frac{\partial\dot{m}}{\partial\rho}\cdot\frac{U_\rho}{\dot{m}}\right)^2 + \left(\frac{\partial\dot{m}}{\partial\dot{\forall}}\cdot\frac{U_{\dot{\forall}}}{\dot{m}}\right)^2\right]^{0.5} = \left[(0.03\%)^2 + (1.0\%)^2\right]^{0.5} = 1.00\%$
2	Temperature difference of fluid from inlet to outlet, $\Delta T = T_{out} - T_{in}$	$\frac{U_{\Delta T}}{\Delta T} = \left[\left(\frac{\partial\Delta T}{\partial T_{out}}\cdot\frac{U_{T_{out}}}{\Delta T}\right)^2 + \left(\frac{\partial\Delta T}{\partial T_{in}}\cdot\frac{U_{T_{in}}}{\Delta T}\right)^2\right]^{0.5} = \left[\left(\frac{1.02}{5.5}\right)^2 + \left(\frac{1.02}{5.5}\right)^2\right]^{0.5} = 26.23\%$
3	Heat transfer, $\dot{Q} = \dot{m}c_p\Delta T$	$\frac{U_{\dot{Q}}}{\dot{Q}} = \left[\left(\frac{\partial\dot{Q}}{\partial\dot{m}}\cdot\frac{U_{\dot{m}}}{\dot{Q}}\right)^2 + \left(\frac{\partial\dot{Q}}{\partial c_p}\cdot\frac{U_{c_p}}{\dot{Q}}\right)^2 + \left(\frac{\partial\dot{Q}}{\partial\Delta T}\cdot\frac{U_{\Delta T}}{\dot{Q}}\right)^2\right]^{0.5} = \left[(1.0\%)^2 + (0.1\%)^2 + (26.23\%)^2\right]^{0.5} = 26.25\%$

rate, 95 °C for cooling fluid inlet temperature, 2.55 m/s air velocity, 24.2 °C for air inlet temperature (Fig. 8).
2. The cause of decreasing at the heat transfer rate while the fluid and the air flow rate increases is that the inlet temperature of the air increases during the comparison between two fluids since the setup was not in a climatized environment (Fig. 8).
3. It has not been observed a remarkable increase in the pressure drop (Fig. 10).
4. It has been seen that the outlet temperature of the coolant decreases by using the nanofluid according to the base fluid [Fig. 9].
5. It has been estimated that the cooling capacity of a car radiator increases not due to enhancement at the overall heat transfer coefficient, due to the temperature difference increase between the surface of the radiator channel and the air. For the nanofluid has high thermal conductivity according to the base fluid, the surface temperature of the channel increases [Fig. 9].
6. Average Nusselt number is calculated for base and nano fluids. As can be seen in Table 8 that average Nusselt number of nanofluids were obtained 11–18% bigger than base fluids ones.
7. The pressure drop between 50% EG–Water based Al_2O_3 nanofluid and 50% EG–Water is shown in the Fig. 10. Assuming the maximum pressure drop is at 25 L/min that calculates approximately 0.83 W as additional pumping power by using Eq.(17). however, the cooling load increase at the same flow rate is approximately 400 W (Figs. 3 and 8).

4.3 Uncertainty analysis

The uncertainty analysis can be separated two sections: a) The uncertainty of a directly measured variable such as temperature, pressure, flow rate and b) the uncertainty of an indirectly measured variable such as heat transfer rate. In this study, the experimental uncertainties were estimated using the method proposed by Kline and McClintock [40]. The maximum uncertainty in heat transfer rate and pressure drop was found to be 26.25% and 12.73%, respectively that are given in Tables 9 and 10.

5 Conclusions

In this study, the heat transfer rate and the pressure drop of a car radiator has been experimentally investigated under the specific conditions by using two different coolant. Those coolants are the nanofluid that consists of 50% ethylene glycol–water mixture including Al_2O_3 nanoparticles with 0.5% by volume and 50% ethylene glycol–water mixture. Using of nanofluids as coolant fluid in the radiator an important increment of cooling capacity of radiator at all of air velocity that can be obtained. Moreover, pressure drop of the radiator was not affected by using nanofluid. All datas are obtained by experiments. However, in the case of testing radiator on the vehicle, different increment of cooling performance can be obtained. But, stable nanofluids are correctly chosen as coolant fluid in the radiators, cooling capacity of its are always increased.

Acknowledgments This project was supported by "The Scientific and Technological Research Council Of Turkey" (TUBITAK 1505, Project No. 5140013) and Kale Oto Radyatör Sanayi ve Ticaret A.Ş. The authors gratefully acknowledge the financial supports provided by TUBITAK and Kale Oto Radyatör.

References

1. Şahin, B., Çomaklı, K., Çomaklı, Ö., Yılmaz, M., Nanoakışkanlar ile ısı transferinin iyileştirilmesi (Heat transfer rate improvement with nanofluids). Mühendis ve Makina, Cilt: 47, Sayı: 559, Sf: 29–34, 2006.
2. Saidur R, Leong KY, Mohammad HA (2011) A review on applications and challenges of nanofluids. Renew Sust Energ Rev 15: 1646–1668
3. Choi SUS, Eastman JA (1995) Enhancing thermal conductivity of fluids with nanoparticles. International Mechanical Engineering Congress & Exposition, San Francisco
4. The other areas of utilization of nanofluids: NanoHEX Report Summary, cordis.europa.eu/project/rcn/92594_en.html, Access Date: 04.02.2017.
5. Kılınç F (2015) Oto radyatörlerde nanoakışkan kullanılarak ısı aktarım performansının arttırılması (Enhancement of heat transfer performance by using nanofluid in auto radiators). Cumhuriyet University, Institute of Natural Sciences, Department of Mechanical Engineering, PhD Thesis
6. Güler KG (2014) Computational modeling of fin-and-tube type vehicle radiators based on porous medium approach. Middle East Technical University, Institute of Natural Sciences, Department of Mechanical Engineering, Master's Thesis
7. The efficiency of the car engines: www.maplesoft.com/support/help/Maple/view.aspx?path=applications/RadiatorDesign, Access Date: 04.02.2017.
8. Sharma, K.V., Sarma, P.K., Azmi, W.H., Mamat, R., Kadirgama, K. (2012) Correlations to predict friction and forced convection heat transfer coefficients of water based nanofluids for turbulent flow in a tube. IJMNTFTP, Vol. 3, No. 4.
9. Kulkarni DP, Vajjha RS, Das DK, Oliva D (2008) Application of aluminum oxide nanofluids in diesel electric generator as jacket water coolant. Appl Therm Eng 28:1774–1781
10. Witry A, Al-Hajeri MH, Bondok AA (2005) Thermal performance of automotive aluminium plate radiator. Appl Therm Eng 25:1207–1218
11. Çetin S (2009) Motorlu taşıt radyatörlerinde kullanılan panjur tip kanatlarda ısı transferi ve akışının incelenmesi (Inspection of the heat transfer and flow in the louvered fins used in the vehicle radiators). Kocaeli University, Institute of Natural Sciences, Department of Mechanical Engineering, Master's Thesis
12. Canbolat AS, Türkan B, Yamankaradeniz R, Can M, Etemoğlu AB (2014) Automobile radyatörlerinde boru sayısının ısıl performansa ve etkenliğe etkisinin incelenmesi (Investigation of the effect of the tube number auto radiators on thermal performance and effectiveness). 7. Otomotiv Teknolojileri Kongresi, Bursa, 1–6
13. Choi S (2006) Nanofluids for improved efficiency in cooling systems. Argonne National Laboratory, April 18–20, 2006.

14. Elias MM, Mahbubul IM, Saidur R, Sohel MR, Shahrul IM, Khaleduzzaman SS, Sadeghipour S (2014) Experimental investigation on the thermo-physical properties of Al2O3 nanoparticles suspended in car radiator coolant. International Communications in Heat and Mass Transfer 54:48–53
15. Sankar BR (2012) Experimental investigations on the performance of Al2O3-water nanofluid as radiator coolant in an automobile engine. Andhra University, College of Engineering, Department of Mechanical Engineering, PhD Thesis
16. Ali HM, Ali H, Liaquat H, Maqsood HTB, Nadir MA (2015) Experimental investigation of convective heat transfer augmentation for car radiator using ZnO-water nanofluids. Energy 84:317–324
17. Bhimani, V.L., Rathod, P.P., Sorathiya, A.S. (2013) Experimental study of heat transfer enhancement using water based nanofluids as a new coolant for car radiators. International J of Emerging Tech and Adv Engineering, Volume 3, Issue 6.
18. Bhogare RA, Kothawale BS (2014) Performance investigation of automobile radiator operated with Al2O3 based nanofluid. IOSR Journal of Mechanical and Civil Engineering 11(3):23–30
19. Heris SZ, Shokrgozar M, Poorpharhang S, Shanbedi M, Noie SH (2014) Experimental study of heat transfer of a car radiator with CuO/ethylene glycol-water as a coolant. J Dispers Sci Technol 35:677–684
20. Hussein AM, Bakar RA, Kadirgama K, Sharma KV (2014) Heat transfer enhancement using nanofluids in an automotive cooling system. International Communications in Heat and Mass Transfer 53:195–202
21. Leong KY, Saidur R, Kazi SN, Mamun AH (2010) Performance investigation of an automotive car radiator operated with nanofluid-based coolants (nanofluid as a coolant in a radiator). Appl Therm Eng 30:2685–2692
22. Vermahmoudi Y, Peyghambarzadeh SM, Hashemabadi SH, Naraki M (2014) Experimental investigation on heat transfer performance of Fe2O3/water nanofluid in an air-finned heat exchanger. European Journal of Mechanics B/Fluids 44:32–41
23. Peyghambarzadeh SM, Hashemabadi SH, Naraki M, Vermahmoudi Y (2013) Experimental study of overall heat transfer coefficient in the application of dilute nanofluids in the car radiator. Appl Therm Eng 52:8–16
24. Kayhani MH, Soltanzadeh H, Heyhat MM, Nazari M, Kowsary F (2012) Experimental study of convective heat transfer and pressure drop of TiO2/water nanofluid. International Communications in Heat and Mass Transfer 39(3):456–462
25. Kayhani MH, Nazari M, Soltanzadeh H, Heyhat MM, Kowsary F (2012) Experimental analysis of turbulent convective heat transfer and pressure drop of AI 2 O 3/water nanofluid in horizontal tube. IET Micro & Nano Letters 7(3):223–227
26. Duangthongsuk W, Wongwises S (2010) An experimental study on the heat transfer performance and pressure drop of TiO2-Water nanofluids flowing under a turbulent flow regime. Int J Heat Mass Transf 53:334–344
27. Nazari M, Karami M, Ashouri M (2014) Comparing the thermal performance of water, Ethylene Glycol, Alumina and CNT nanofluids in CPU cooling: Experimental study. Exp Thermal Fluid Sci 57:371–377
28. Nazari M, Ashouri M, Kayhani MH, Tamayol A (2015) Experimental study of convective heat transfer of a nanofluid through a pipe filled with metal foam. Int J Therm Sci 88:33–39
29. Maghrebi MJ, Nazari M, Armaghani T (2012) Forced convection heat transfer of nanofluids in a porous channel. Transp Porous Media 93(3):401–413
30. Sandhya D, Reddy MCS, Rao VV (2016) Improving the cooling performance of automobile radiator with ethylene glycol water based TiO2 nano fluids. International Communications in Heat and Mass Transfer 78:121–126
31. Oliveira GA, Contreras EMC, Filho EPB (2017) Experimental study on the heat transfer of MWCNT/water nanofluid flowing in a car radiator. Appl Therm Eng 111:1450–1456
32. Emerald N., Lazarus G., Ramachandran K., Brusly S., Gnana S. (2018) Heat transfer performance of a compact loop heat pipe with alumina and silver nanofluid. J Therm Anal Calorim. https://doi.org/10.1007/s10973-018-7739-0.
33. Kale Oto Radyatör Sanayi ve Ticaret A.Ş., Kocaeli, Turkey.
34. Touloukian Y.S, Powell RW, Ho CY, Klemens PG (1970) Thermophysical properties of matter: The TPRC (Thermophysical Properties Research Center) Data Series. Volume 2, Purdue University, 97
35. Touloukian, Y.S., Buyco, E.H., Thermophysical properties of matter: The TPRC (Thermophysical Properties Research Center) Data Series. Volume 5, Purdue University, 24–27, 1970.
36. Topuz A, Engin T, Özalp AA, Erdoğan B, Yurduseven S, Mert S, Perut A (2016) Preparation and stability analysis of water based Al2O3, TiO2 and ZnO nanofluids. International Conference on Engineering and Natural Sciences, Sarajevo 610–621
37. Topuz A, Engin E, Özalp, Erdoğan B, Mert S, Yeter A (2018) Experimental investigation of optimum thermal performance and pressure drop of water-based Al_2O_3, TiO_2 and ZnO nanofluids flowing inside a circular microchannel. J Therm Anal Calorim 131(3):2843–2863
38. Erdoğan B (2016) Mini/mikro kanallarda nanoakışkan ile ısı transferinin deneysel Incelenmesi (Experimental Investigation of Heat Transfer of Nanofluids Flowing Inside A Circular Mini/Microchannels), Zonguldak Bülent Ecevit Üniversitesi, Institute of Natural Sciences, Department of Mechanical Engineering, PhD Thesis
39. Mert S (2017) Otomobil Radyatörlerinde Nanoakişkan Kullanimi (Nanofluid Usage In Automobile Radiators). Sakarya University, Institute of Natural Sciences, Department of Mechanical Engineering, Master Thesis
40. Holman JP (2012) Experimental methods for engineers, 8th edn. McGraw-Hill, New York